Vehar, G. A., Keyt, B., Eaton, D., Rodriguez, H., O'Brien, D. P., Rotblat, F., Opperman, H., Keck, R., Wood, W. I., Harkins, R. N., Tuddenham, E. G. D., Lawn, R. M., & Capon, D. (1984) *Nature (London) 312*, 337.
Weinstein, M., Chute, L., & Deykin, D. (1981) *Proc. Natl. Acad. Sci. U.S.A. 78*, 5137.
Weiss, H. J., Sussman, I. I., & Hoyer, L. W. (1977) *J. Clin. Invest. 60*, 390.
Weiss, H. J., Baumgartner, H. R., & Tschopp, T. B. (1978) *Blood 51*, 267.

Complete Assignment of the Imino Protons of *Escherichia coli* Valine Transfer RNA: Two-Dimensional NMR Studies in Water†

Dennis R. Hare, N. Susan Ribeiro, David E. Wemmer, and Brian R. Reid*
Departments of Chemistry and Biochemistry, University of Washington, Seattle, Washington 98195
Received October 12, 1984

ABSTRACT: The imino proton spectrum of *Escherichia coli* valine tRNA has been studied by two-dimensional nuclear Overhauser effect spectroscopy (NOESY) in H_2O solution. The small nuclear Overhauser effects from the imino proton of an internal base pair to the imino protons of each nearest neighbor can be observed as off-diagonal cross-peaks. In this way most of the sequential NOE connectivity trains for all the helices in this molecule can be determined in a single experiment. AU resonances can be distinguished from GC resonances by the AU imino NOE to the aromatic adenine C2-H, thus leading to specific base-pair assignments. In general, the NOESY spectrum alone is not capable of assigning *every* imino proton resonance even in well-resolved tRNA spectra. Multiple proton peaks exhibit more than two cross-peaks, resulting in ambiguous connectivities, and coupling between protons with similar chemical shifts produces cross-peaks that are incompletely resolved from the diagonal. The sequence of the particular tRNA determines the occurrence of the latter problem, which can often be solved by careful one-dimensional experiments. The complete imino proton assignments of *E. coli* valine tRNA are presented.

The hydrogen-bonded imino protons of helical nucleic acids offer two major advantages in the analysis of nucleic acid structure and dynamics by high-resolution NMR.[1] First, the imino protons resonate in a uniquely low-field region of the spectrum, and there is only one such proton per Watson–Crick pair. Second, their exchange with solvent requires some form of transient opening of the corresponding base pair (Teitelbaum & Englander, 1975), and this makes them potentially very useful in monitoring nucleic acid dynamics by NMR. In order to accurately interpret helix–coil dynamics at various positions in a nucleic acid such as tRNA, one obviously needs to be able to assign each low-field imino proton resonance to its specific base pair. However, imino proton assignments have previously been made by a variety of indirect methods, often with conflicting results, and this has complicated the interpretation of dynamic studies on these molecules. Earlier indirect assignment strategies include hairpin fragment studies (Lightfoot et al., 1973), empirically calibrated ring-current shift estimates (Shulman et al., 1973; Kearns, 1976; Reid et al., 1979), chemical modification (Salemink et al., 1977; Hurd & Reid, 1979), theoretical ring-current shift calculations (Robillard et al., 1976), and paramagnetic ion binding (Hurd et al., 1979), all of which require prior assumptions about the solution structure of the molecule. In a somewhat different approach, the first resonances to melt upon raising the temperature of the tRNA were assigned to tertiary base pairs on the unproven assumption that tertiary folding is the most labile part of the tRNA solution structure (Hilbers & Shulman, 1974; Romer & Varadi, 1977).

The development of FTNMR in H_2O solution and the application of double-resonance methods to exchangeable protons by Redfield and colleagues (Redfield, 1978; Johnston & Redfield, 1977) ushered in a new era of nucleic acid research in which imino protons could be directly assigned by means of dipolar proton–proton coupling, i.e., the nuclear Overhauser effect or NOE. In this technique the resonance of interest is selectively saturated; surrounding protons within 4–5 Å become partially cross-saturated and appear as smaller peaks in the difference spectrum. With this technique Redfield and coworkers originally identified the two strongly coupled imino protons within a GU wobble base pair (Johnston & Redfield, 1978) and subsequently identified the imino protons of the two intervening Watson–Crick neighbors between the two wobble pairs in the dihydrouridine helix of $tRNA^{Asp}$ (Roy & Redfield, 1981). Sequential NOE connectivities have been used to assign the imino protons of consecutive Watson–Crick pairs in entire helices in various tRNAs (Hare & Reid, 1982a,b; Heerschap et al., 1982); extension of this technique has led to the complete assignment of all imino protons in *Escherichia coli* isoleucine tRNA and valine tRNA (Hare, 1983) and in yeast phenylalanine tRNA (Roy & Redfield, 1983; Heerschap et al., 1983a,b). However, Heerschap et al. differ from Roy and

† This work was supported by Grant PCM-8215812 from the National Science Foundation and Grant GM28764 from the National Institutes of Health and an instrumentation grant from the Murdock Foundation.
* Address correspondence to this author at the Department of Chemistry.

[1] Abbreviations: NMR, nuclear magnetic resonance; NOE, nuclear Overhauser effect; NOESY, two-dimensional nuclear Overhauser effect spectroscopy; tRNA, transfer ribonucleic acid; T, ribothymidine; D, dihydrouridine; FTNMR, Fourier-transform nuclear magnetic resonance.

0006-2960/85/0424-4300$01.50/0

Redfield in their assignments of three or four resonances in yeast phenylalanine tRNA. In the one-dimensional NOE technique, the selective irradiation of each imino resonance in turn is somewhat laborious, and problems of selectivity are often encountered when two imino resonances are insufficiently resolved to permit irradiation of one without also saturating the other.

The last few years have seen a great increase in the application of two-dimensional NMR to biological polymers such as proteins and nucleic acids (Wuthrich et al., 1982; Wagner & Wuthrich, 1982; Scheek et al., 1983; Hare et al., 1983; Wemmer et al., 1984). In a two-dimensional NOE or NOESY experiment, the nuclear spins become frequency labeled by evolving during a variable time period between two pulses. Subsequently, the spins are allowed to cross-relax during a fixed "mixing time", and the system is then sampled with an observation pulse (Macura & Ernst, 1980). After Fourier transformation as a function of both the evolution time and the acquisition time, all pair-wise NOEs can, in principle, be revealed simultaneously in the resulting two-dimensional map.

The ability to carry out two-dimensional NOE spectra on the relatively rapidly exchanging imino protons of tRNA or DNA presents an extra challenge in that suppressing the large solvent peak by selective saturation of the water resonance leads to the obliteration of the imino protons of interest by spin diffusion and/or chemical exchange. Haasnoot & Hilbers first attempted two-dimensional NOESY experiments on the imino protons of a helical DNA hairpin by using standard "hard" pulses to perturb the spins and a time-shared "tailored" pulse sequence (combined with data-shift accumulation) for selective observation (Haasnoot & Hilbers, 1983). However, they found no NOE cross-peaks between imino protons because of inadequate signal-to-noise ratios and thus could not assign any imino protons from the NOESY spectrum. Imino–imino cross-peaks were subsequently observed in the NOESY spectrum of yeast phenylalanine tRNA by the same pulse sequence (Haasnoot et al., 1983), and some of the assignments made previously by one-dimensional NOE were corroborated from the NOESY map; although a few cross-peak connectivities could be made (e.g., 14–13, 11–10, 6–5), the number of observed cross-peaks fell far short of that expected for 27 imino protons, and sequential connectivities from one end of a helix to the other could not be made from the two-dimensional spectrum, even for the short dihydrouridine stem (Hilbers et al., 1983). In this paper we present the results of a soft-pulse NOESY experiment that reveals almost all the imino–imino NOEs between tRNA base pairs in a single experiment. From the NOESY map, most of the imino protons can be uniquely assigned by sequential connectivity with significant time saving compared to one-dimensional methods; the resulting assignments agree with those from one-dimensional NOEs obtained by selective saturation of each resonance (Hare, 1983).

Materials and Methods

E. coli $tRNA_1^{Val}$ was purified from crude *E. coli* B tRNA by sequential chromatography on BD-cellulose, DEAE-cellulose, and then Sepharose 4B as previously described (Reid et al., 1977, 1979). The final purified tRNA was dialyzed extensively against two changes of 12 L of distilled water and lyophilized. The pure isoacceptor $tRNA_1^{Val}$ accepted 1780 pmol of [^{14}C]valine/A_{260} unit when aminoacylated with partially purified valyl-tRNA synthetase.

Two-dimensional NMR spectroscopy was carried out at 500 MHz on a Bruker WM500 spectrometer with 50 mg of dialyzed, lyophilized tRNA dissolved in 10 mM sodium phosphate buffer, pH 7.0, to a final volume of 0.45 mL (tRNA concentration ca. 4.5 mM). In the NOESY spectra, two soft Alexander long pulses centered at 12.5 ppm and nulled at the H_2O frequency were used for frequency labeling followed by a mixing time of 0.12 s and a Redfield 21412 observation pulse of 253 μs offset 3950 Hz from the water resonance. The advantage of this method of suppressing water in two-dimensional NMR is that, with a relaxation delay of 0.1 s, the entire duty cycle is only 0.4 s and the entire NOESY data set can be collected in approximately 16 h. The initial t_1 delay was set at 0.9 μs, and 256 t_1 spectra incremented by 0.037 ms were collected in 1K channels; pulses were cycled by standard magnitude NOESY phase cycling (Macura et al., 1981). Since imino line widths are 20–30 Hz, the signal had virtually disappeared after about 250 t_1 increments due to the short t_2, and so, only 256 t_1 points were collected. Each t_1 experiment was signal averaged for 562 pulses (ca. 3.75 min). The data set was immediately transferred to a VAX 11/780 computer and Fourier transformed in two dimensions with a skewed sine-bell apodization (skew = 1.3)[2] in both dimensions with our own 2DFT software. The t_2 transform was performed in 1K complex points, and after transformation, the upfield half of the data set was discarded. The t_1 data were zero filled to 1K complex points, and after Fourier transformation, the upfield half was also discarded, resulting in a 512 × 512 matrix of real data points with a digital resolution of 6.7 Hz per point. The NOESY data were processed and plotted as contour maps in the absolute magnitude mode on a Zeta plotter interfaced to the VAX.

For the one-dimensional spectrum shown in Figure 5, a 10-mg aliquot of tRNA was further dialyzed at 4 °C against 5 mM EDTA and then against distilled water to partially remove residual-bound magnesium. The sample was then lyophilized to dryness and dissolved directly in 0.4 mL of 10 mM sodium phosphate, pH 7.0 (tRNA concentration ca. 1 mM). This procedure was found to produce optimal resolution between the two components in the double-intensity peaks CD, EF, PQ, RS, and TT′. However, the magnesium is not completely removed by this procedure in that the resulting spectrum most closely resembles that in Figure 2c of our previous study on magnesium effects on $tRNA_1^{Val}$ (Reid et al., 1979).

Results

The two-dimensional NOE (NOESY) spectrum of the imino proton spectral region of *E. coli* $tRNA_1^{Val}$ in H_2O at 27 °C is shown in Figure 1, and the cloverleaf sequence of this molecule is shown in Figure 5. The water-dialyzed pure tRNA, containing 2–3 mol of residual bound magnesium per mol of tRNA, was lyophilized and directly dissolved in 10 mM phosphate buffer to a final tRNA concentration of 4–5 mM. At these relatively high concentrations the sample is slightly viscous, leading to somewhat broader line widths and less resolution than in our previously published spectra of this tRNA (Hare & Reid, 1982a), but all of the corresponding imino resonances are still recognizable in the one-dimensional spectrum. The two-dimensional data were processed in the absolute magnitude mode, leading to even broader line shapes and less resolution of the spectrum on the diagonal. Nevertheless there are 17 well-resolved off-diagonal cross-peaks and

[2] A skewed sine bell function is defined as

$$y_i = \sin [\delta + (\pi - \delta)(i/n)^k]$$

where δ is the phase shift in radians, n is the number of points in the window, i is the data point, and k is the skew value (D. R. Hare and D. E. Wemmer, unpublished results).

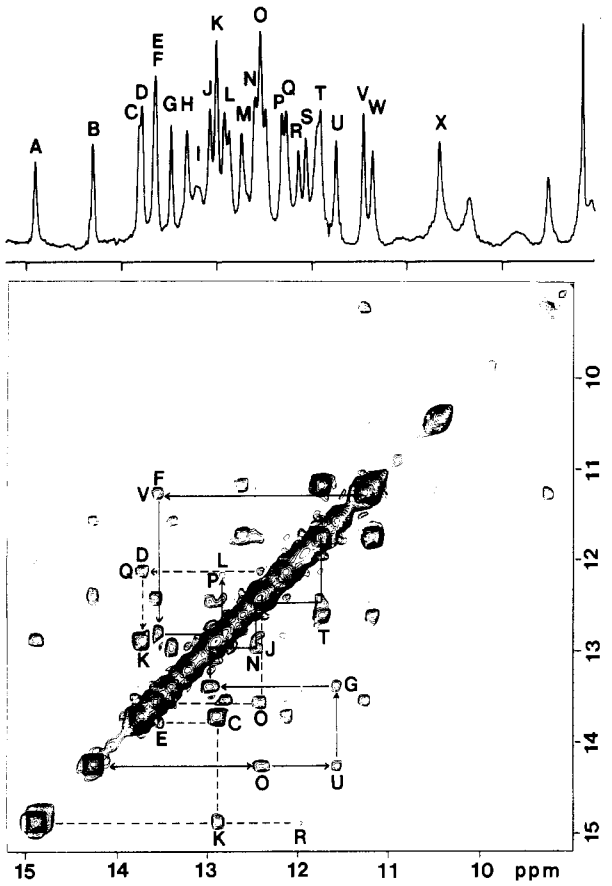

FIGURE 1: Low-field region of the NOESY spectrum of *E. coli* $tRNA_1^{Val}$ at 27 °C in H_2O showing the imino–imino NOEs. In the lower right sector the connectivity traces of the acceptor helix and dihydrouridine helix are shown as solid and dotted lines, respectively. The one-dimensional spectrum at the top is that of a separate sample treated similarly to the NOESY sample. However, in the NOESY sample the two protons in peak EF are partially resolved whereas the two protons in peak T have coalesced.

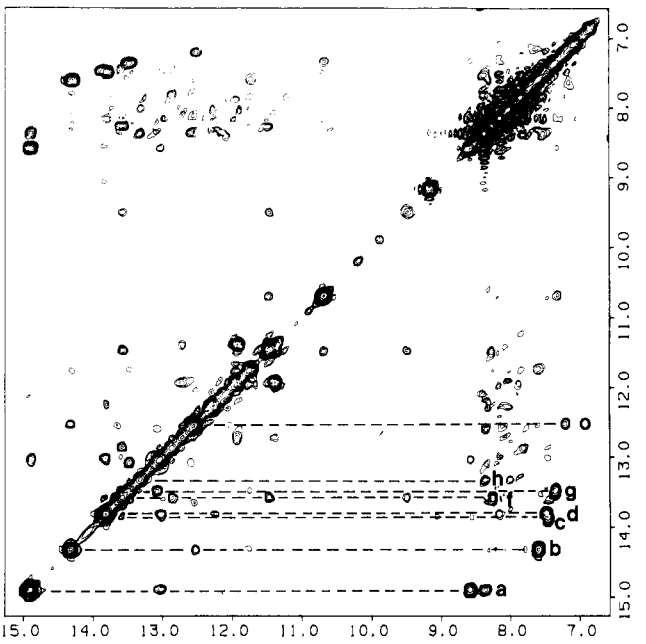

FIGURE 2: NOESY spectrum of *E. coli* $tRNA_1^{Val}$ at 32 °C showing the imino and aromatic proton regions. AU-type imino protons have been connected horizontally by a dotted line to the cross-peak of their proximal C2-H or C8-H in the 7–9 ppm region, which has been labeled with the corresponding lower-case letter.

eight additional cross-peaks closer to the diagonal, reflecting a potential of 25 discernible imino–imino NOEs for the 27 imino protons between 11 and 15 ppm. The NOE between two imino protons effectively identifies them as nearest neighbors as discussed elsewhere (Johnston & Redfield, 1981; Hare & Reid, 1982a,b).

The imino proton peaks of $tRNA_1^{Val}$ are labeled alphabetically from A to X according to our previous convention (Hare & Reid, 1982a). In the lower right triangle of the NOESY spectrum in Figure 1, one chain of connectivity has been drawn in solid lines and another in dashed lines. Starting from the single proton B, it is obvious that its two neighbors are U (a single proton) and O (a multiple proton peak). The sequential connectivity from U to G to J to N to T is traced by the solid line in the lower right triangle. G is a single proton, J is a partially resolved single proton, N is a shoulder on the downfield side of the complex N/O peak containing at least four protons, and T contains two protons. Thus, the spatially connected resonances OBUGJNT all reside within the same helix, and the fact that they represent seven base pairs makes the acceptor helix a leading candidate. The chemical shifts of peaks T, N, and J are in the region where AU pairs are not normally found, suggesting that they are probably GC-1, GC-2, and GC-3, respectively. However, at the other end of this helix peak O at 12.55 ppm is at an anomalously high-field position for typical AU protons, which we and others have generally found to resonate in the 13–14.5 ppm region. Nevertheless, we have confirmed that peak O indeed contains an upfield-shifted AU pair by making use of the NOE from the imino proton to the narrow C2-H of adenine in the 7–8 ppm region, which differentiates AU pairs from GC pairs (Hare & Reid, 1982b). Figure 2 shows a NOESY spectrum at 32 °C from which it can be seen that peaks B, C, D, G, and O exhibit adenine C2-H NOEs in the 7–8 ppm region thus accounting for the five Watson–Crick AU pairs in $tRNA_1^{Val}$. Peaks A, F, and H exhibit lower field aromatic NOEs in the 8–9 ppm region. We have previously shown that, in DNA, the more deshielded purine C8-H protons generally occur in the 8–9 ppm region (Wemmer et al., 1984), and in agreement with this, sequential NOE connectivities shown later indicate that cross-peaks a, f, and h are C8-H NOEs from imino protons A, F, and H hydrogen bonded to N7 of purines in Hoogsteen base pairing. Note that the two-proton peak EF gives only one aromatic CH NOE, indicating that the second imino proton in this peak is a GC pair. Thus, the OBUGJNT connectivity consists of base pairs of the type AU, AU, GC, AU, GC, GC, and GC and obviously corresponds to base pairs 7, 6, 5, 4, 3, 2, and 1. From separate studies on dynamics and melting, we have shown that UA-7, in addition to its surprising chemical shift, is also a rather labile hydrogen bond and this may be related to its upfield residence in peak O.

The single resonance A is another convenient independent starting point for sequential imino assignments in that its intensity directly reflects the level of thiolation at uridine 8, thus leading to its unequivocal assignment as the imino proton of the s^4U-8-A-14 tertiary Hoogsteen base pair (Hare & Reid, 1982a). As traced by the dashed line in Figure 1, A is adjacent to K, which we have previously assigned to CG-13 (Hare & Reid, 1982a)—peak K contains two protons. Peak A also gives a weaker, but quite reproducible, NOE to R (see also Figure 6), which we assign to the tertiary base pair 15–48 (a reverse Watson–Crick GC pair) located on the other side of the 8–14 pair in the crystal structure of yeast $tRNA^{Phe}$ (Klug et al., 1974; Kim et al., 1974). Thus, peak K contains CG-13 and another base pair and hence should exhibit three more cross-peaks besides the AK cross-peak. However, there is only

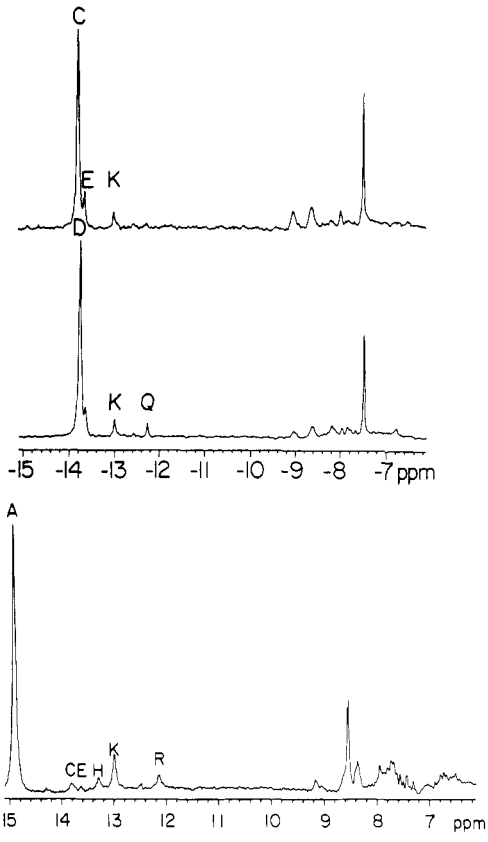

FIGURE 3: One-dimensional NOEs produced by selective saturation of peaks C, D, and A. Although D and E are closer in frequency, the effect of D on E is less than the effect of C on E, thus demonstrating the low level of irradiation spillover and proving that the effect on E is a real NOE from peak C. In the lower spectrum, peak A was continuously saturated for 1.5 s; in addition to peaks K and R (seen at shorter irradiation times), cross-saturation of peaks C and H (and a weaker effect on E) are now seen as a result of extensive spin–diffusion.

one other well-resolved cross-peak from K, but this 13.8 ppm cross-peak is doubly intense and encompasses both the C and D components of the poorly resolved two-proton CD peak. Thus, it appears possible, even likely, that one of the protons in peak K is adjacent to C while the other is adjacent to peak D. One of the K protons is CG-13 while the other is an unknown GC pair and both C and D are AU pairs. Peak C (the downfield side of CD) appears to be coupled to peak E (the downfield side of EF) via a marginally resolved cross-peak close to the diagonal (Figures 1 and 2). At lower magnesium ion concentrations, peaks E and F resolve into two single protons (see Figure 5), and under these conditions peak E can be shown to be a GC pair with a somewhat downfield chemical shift. Under these conditions it is E, not F, that is coupled to C. However at this stage the resolution in the two-dimensional spectrum is inadequate to trace a unique path through this part of the molecule, and we have had to resort to one-dimensional NOE spectra to resolve this ambiguity.

Figure 3 shows the results of three strategic NOEs that were essential in unambiguously identifying the resonances of the dihydrouridine helix. Under somewhat lower magnesium ion conditions, the two protons in peak CD separate slightly (see Figure 5); under these conditions selective irradiation of the left side of peak C cross-saturates K and E, although the latter peak is only 70 Hz away and the effect might possibly be due to direct irradiation spillover. However, irradiating peak D cross-saturates Q and K′, and the fact that D, which is closer to E in chemical shift, excites E *less* than C does confirms that the NOE from C to E is real and not due to a spillover artifact. Thus, spatially the AU resonance C resides between K and E (both GC pairs) whereas the AU resonance D resides between K′ and Q (also both GC pairs). To decide whether the KCE set or the K′DQ set is base pairs 13, 12, and 11, we irradiated peak A (the 8–14 pair) for 1.5 s to deliberately allow spin–diffusion to cross-saturate several resonances in the dihydrouridine helix. As shown in Figure 3, peak A exhibits second-order NOEs to peak C (and also E) via CG-13, thus establishing that A, K, C, and E correspond to base pairs 14, 13, 12, and 11. The A to R NOE is also now much stronger in this steady-state experiment than the transient NOE in the NOESY map, and peak H also appears to be close to s^4U-8-A-14 and CG-13.

Returning to the NOESY map, there is a well-resolved E to O cross-peak thus assigning GC-10 to one of the protons in peak O. The K to H cross-peak is also apparent at 27 °C. The fact that peak H gives only one NOE, which places it close in space to CG-13, leads us to assign peak H to the imino proton of m^7G-46, which is hydrogen bonded to the guanine N7 of CG-13 in the crystal structure of yeast $tRNA^{Phe}$ (Klug et al., 1974; Kim et al., 1974). This assignment agrees with our previous assignment of this resonance on the basis of chemical removal of m^7G-46 (Hurd & Reid, 1979). Thus at this stage we can assign RAKCEO to base pairs 15, 14, 13, 12, 11, and 10. The assignment of peak C to UA-12 leaves only one AU pair unassigned, and the adenine C2-H NOEs identify peak D as the remaining AU pair. We have now assigned 14 resonances including the acceptor and dihydrouridine helices and three tertiary resonances.

Now that the acceptor and dihydrouridine helices have been assigned, the two remaining unassigned helices are the anticodon stem and the ribothymidine stem. The anticodon stem contains the remaining AU pair, namely, UA-29, identified as peak D on the basis of its adenine C2-H NOE at 7.45 ppm. The neighbors of peak D are obviously Q and K′ as shown by the dotted line in the upper half of Figure 1 and the one-dimensional NOEs in Figure 3. Thus, peaks K and Q contain CG-28 and CG-30, but the anticodon helix is symmetrical with respect to the central UA pair, and it is not possible from first principles to establish which is which. Peak Q has a well-defined NOE to peak O, which must be either CG-27 or CG-31, whereas peak K exhibits a weak, close to the diagonal, NOE to the labile proton I. Thus, the anticodon helix is represented by the connectivity train IKDQO, but the symmetry of this helix does not permit the orientation to be established independently. To orient this connectivity train we have had to resort to arguments based on the geometry of RNA helices. On the reasonable assumption that the the anticodon helix is right-handed and close to the A′ helical pitch, one would expect the imino proton of CG-30 to be more upfield shifted by the strong ring current of A41 than would the imino proton of CG-28. On this basis we assign peak Q at 12.25 ppm to CG-30 and peak K at 13 ppm to CG-28. Although we have made no attempt to quantitatively evaluate the ring-current shifts, these relative values agree qualitatively with published ring-current shift estimates for A′ RNAhelices (Arter & Schmidt, 1976). Thus, without direct experimental proof, we conclude that the connected sequence I, K, D, Q, O corresponds to base pairs 27, 28, 29, 30, and 31 rather than the other way around.

Only the thymine helix now remains unassigned, and 10 of the 29 protons between 10.5 and 15 ppm have not been assigned to their specific base pairs; these resonances are peaks F, L, L′, M, P, S, T′, V, W, and X. The thymine helix contains two convenient, readily identifiable base pairs from which to

begin assignments. These are the GU wobble base pair in position 50, and the tertiary T-54-A-58 Hoogsteen pair; the rest of this helix consists of GC pairs. Peak F, with its C8-H NOE at 8.3 ppm is the last N3-H remaining unassigned and is the obvious candidate for the T-54 imino proton at the end of this helix. Peak F shows two well-resolved NOEs and obviously resides between peaks V and L, as shown by the solid line in the upper part of Figure 1. Under the conditions of the Figure 1 NOESY map, peaks E and F are almost perfectly superimposed, but we have previously shown (Reid et al., 1979) that, at lower magnesium and higher temperature, peak F moves upfield and can be resolved from peak E (see Figure 5); under these latter conditions we have confirmed that it is peak F, rather than E, that is coupled to V and L. The T-54-A-58 base pair is formally at the end of the thymine helix with GC-53 and GC-52 stacked on the "inside" of this base pair. On the "outside", the nearest neighbor is Ψ-55. In one direction the observed connectivity chain is F to L to P, whereas in the other direction it is F to V (11.5 ppm) with perhaps a weak NOE from V to X (10.6 ppm). Although marginal in Figure 1, under the conditions of Figure 2 the V to X NOE is much stronger, as is the NOE from X to an aromatic CH resonance at 7.35 ppm and from V to an exchangeable proton at 9.4 ppm. The chemical shifts of peaks V and X virtually exclude their being GC-53 and GC-52, and on this basis, we interpret the FVX connectivity as being on the outside of T-54-A-5 and assign V and X to the two imino protons of Ψ-55. In the other direction, the FLP connectivity assigns peak L to GC-53 (12.9 ppm) and peak P to GC-52 (12.3 ppm). Peak P does not exhibit any additional NOEs besides the weak one to L, and the connectivity beyond GC-52 appears to stop at this point. Fortunately, we have not yet used the GU wobble pair conveniently located at position 50, and this serves to complete the assignment of the interior portion of the thymine helix. The intense imino–imino NOE in a GU pair containing two imino protons was originally exploited by Johnston and Redfield to identify such wobble base pairs (Johnston & Redfield, 1979). From the NOESY maps the intense cross-peaks between peaks T and W immediately identify these as both belonging to GU-50 in complete agreement with our previous assignment of GU-50 by one-dimensional methods (Hurd & Reid, 1979). Peak T and peak W are both strongly coupled to peak M; peak T is also coupled to peak S whereas W is not. Assuming that the thymine helix is right-handed, CG-51 should couple to both imino protons of GU-50 whereas GC-49 should couple only to U-64 of the GU pair. Hence, peak M is CG-51, peak S is GC-49, peak W is G-50, and peak T is U-64. Independent evidence based on the greater deshielding of U N3-H (11.3 ppm) compared to G N1H (10.7 ppm) in Me_2SO, combined with the downfield shift by the G ring current on the U N3-H in a GU pair, corroborates the assignment of U-64 at 11.95 ppm and G-50 at 11.4 ppm. This relative order of deshielding for the two GU imino protons is in agreement with the direct experimental results of Griffey et al. on the GU imino protons of $tRNA^{fMet}$ using ^{15}N labeling (Griffey et al., 1982). CG-51 (peak M) does not appear to be close enough to the imino proton of GC-52 (peak P) to generate an NOE, perhaps due to helix distortion by the neighboring GU wobble base pair.

Because of the lack of a continuous connectivity down the thymine stem, we felt obliged to establish the identities of the base pairs in the exterior portion of this helix by independent methods. The unique thymine methyl resonance at 1.0 ppm is a convenient, independent marker in this section of the molecule and has been exploited by Tropp and Redfield to probe resonances from the T loop (Tropp & Redfield, 1981). They have shown that the T-54 methyl group is coupled to Ψ-55 N1-H in several tRNAs. In an extension of this approach, we subsequently demonstrated that, in $tRNA^{Ile}$, Ψ-55 N1-H is weakly coupled to Ψ-55 N3-H, which further couples to the T-54-A-58 imino proton (Hare & Reid, 1982). We therefore irradiated the thymine methyl resonance for 1 s to allow spin–diffusion to occur throughout this region of the molecule. The results are shown in Figure 4. In addition to strong cross-saturation of peak X (Ψ-55 N1-H), second-order NOEs are also observed to peaks F, L, P, and V. The connectivity sequence is V to F to L to P, thus confirming their assignments to positions 55, 54, 53, and 52.

We have now assigned the nine peaks S, T, W, M, P, L, F, V, and X to the thymine helix and loop. An additional imino proton at 9.4 ppm is obviously close to Ψ-55 and is probably the non-hydrogen-bonded imino proton of G-18. The assignments are summarized by helix in Table I, and Figure 5 shows a resolution-enhanced spectrum under solution conditions designed to effect maximal peak separation, with each resonance labeled according to its base-pair identity. The only unassigned imino proton is peak L′ at 12.9 ppm. This resonance is relatively labile, and we tentatively assign it to the G-19-C-56 tertiary base pair, which, according to the crystal

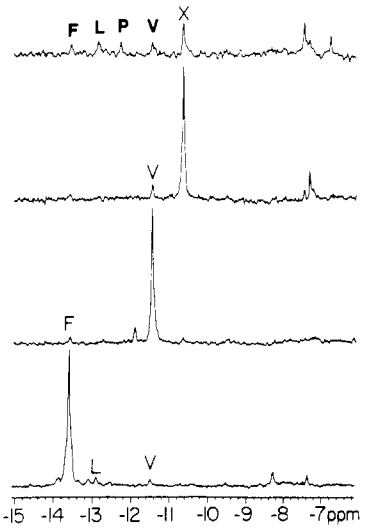

FIGURE 4: One-dimensional NOEs at the loop end of the T helix. The top spectrum shows the effects of saturating the T-54 methyl resonance 1 ppm downfield of DSS. The lower spectra show the connectivity train from X (Ψ-55 N1-H) to V to F to L.

Table I: Base-Pair Assignments for the Imino Protons of $tRNA_1^{Val}$

base pair	peak	base pair	peak
GC-1	T	CG-27	I[b]
GC-2	N	CG-28	K
GC-3	J	UA-29	D
UA-4	G	CG-30	Q
GC-5	U	CG-31	O[b]
AU-6	B	CG-49	S
UA-7	O	GU-50	W, T′
GC-10	O	CG-51	M
CG-11	E	GC-52	P
UA-12	C	GC-53	L
CG-13	K	T-54-A-58[a]	F
s^4U-8-A-14[a]	A	Ψ-55[a]	V, X
G-15-C-48[a]	R	G-19-C-56[a]	L′?
m^7G-46-G-22[a]	H		

[a] Denotes a tertiary base pair. [b] Although unlikely, it is possible that the anticodon helix has been assigned upside down with I being CG-31 and O being CG-27. Chemical shifts are sensitive to ionic strength, temperature, and magnesium ion and, hence, have not been listed.

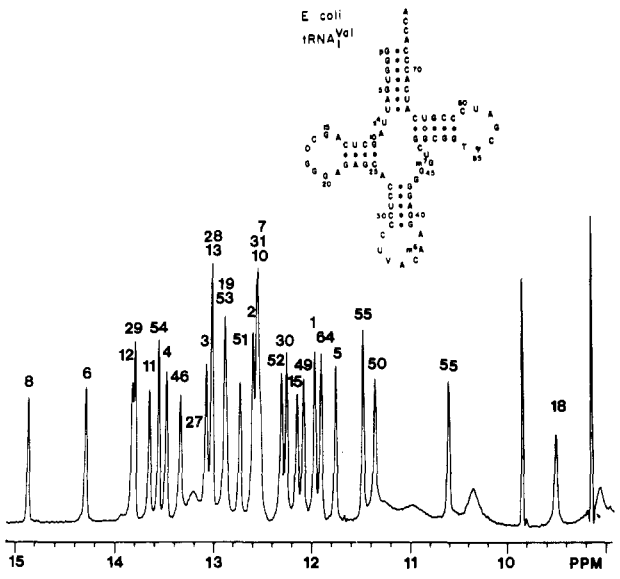

FIGURE 5: Resolution-enhanced imino proton spectrum of *E. coli* $tRNA_1^{Val}$ at 35 °C after partial removal of residual bound magnesium ion to effect maximum peak resolution. Each peak is labeled with its base-pair identity as described in the text.

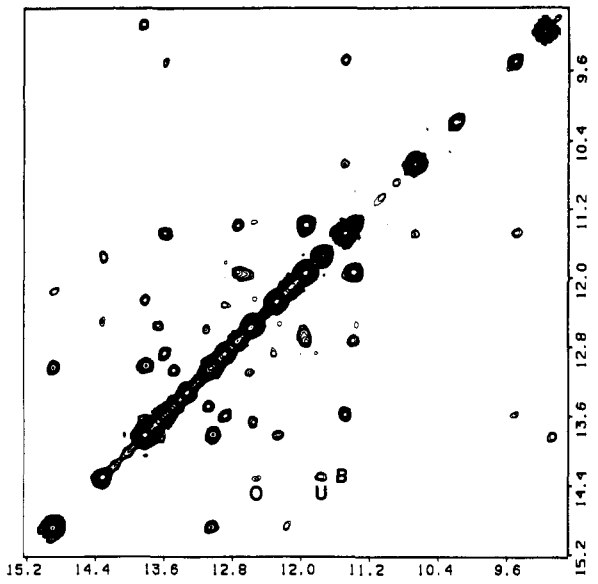

FIGURE 6: Imino proton NOESY spectrum of *E. coli* $tRNA_1^{Val}$ at 37 °C. Note the reduction of the OB cross-peak, the increase in the AR cross-peak, and the disappearance of the UG cross-peak compared to Figure 1.

structure, is exposed to solvent at the periphery of the molecule and is not close enough to any other base pair to exhibit dipolar coupling to other imino protons.

Discussion

We have shown that the two-dimensional NOESY spectrum of a tRNA in H_2O solution can be extremely informative in assigning the hydrogen-bonded imino protons to their respective base pairs. In the present study we chose *E. coli* $tRNA_1^{Val}$ because it presents a fairly well-resolved imino proton spectrum (22 peaks for 27 protons) and because most of the imino–imino NOEs have already been investigated by one-dimensional assignment methods (Hare & Reid, 1982a; Hare, 1983). However, even in such a well-resolved tRNA, it is apparent that a single NOESY spectrum alone cannot lead to unambiguous assignment of *every* imino proton. Two of the major limitations leading to ambiguous connectivity traces are multiple proton peaks with several off-diagonal cross-peaks and NOEs between peaks with similar chemical shifts, which give cross-peaks that are incompletely resolved from the diagonal. An excellent example of both of these problems is the case of the two-proton peak K in which one component gives an NOE to C while the other gives an NOE to D in the two-proton peak C,D; the other neighbor of peak C is E, which is separated by only 0.15 ppm in chemical shift. The NOESY data alone cannot establish whether it is CG-13 or the other proton in peak K that cross-saturates peak C, and in fact, we previously misassigned peak D and its neighbor Q to UA-12 and CG-11, respectively (Hare & Reid, 1982a). To resolve this dilemma, we have now resorted to selective excitation of only the CG-13 component of peak K by cross-saturating it via the 8–14 base pair and made use of spin–diffusion from CG-13 to show that peak C is in fact UA-12. The assignment of UA-12 at 13.8 ppm and CG-11 at 13.65 ppm is now in agreement with the assignment of these two base pairs in the identical D-stem sequence in yeast $tRNA^{Phe}$ (Roy & Redfield, 1983; Hilbers et al., 1983). A further ambiguity arises in the symmetrical anticodon stem, which has CG-28 and CG-27 on one side and CG-30 and CG-31 on the other side of UA-29. From the NOESY map alone one cannot establish which two CG pairs are above and which two are below the central UA pair. Despite these occasional limitations, the NOESY map is extremely useful in assigning most of the imino protons, and the use of the soft-pulse approach appears to be a significant improvement over hard-pulse methods in that sequential NOE connectivities for all four helices in tRNA can now be made.

An interesting aside to the present assignment goals is the temperature dependence of the NOESY map. For instance, raising the temperature by only 5 °C, as shown in Figure 2, reduces the line width and resolves the previously marginal C–E cross-peak from the diagonal. However, it also weakens the B–U cross-peak (AU-6 to GC-5) and the U–G cross-peak (GC-5 to UA-4). A reduced NOE can arise either by washing out the cross-peak by increased imino proton exchange with solvent or by the two imino protons structurally moving apart so that they are no longer effectively dipolar coupled. To investigate this further, we repeated the NOESY experiment at 37 °C, and the results are shown in Figure 6. Now the O–B NOE (UA-7 to AU-6) has weakened, and the U–G NOE (GC-5 to UA-4) has disappeared entirely! It is also worth noting that G-15-C-48 appears to have moved closer to s^4U-8-A-14 (A–R is stronger) and the L–P cross-peak (GC-53 to GC-52) is marginally stronger, corroborating these originally somewhat tenuous cross-peaks. The solvent exchange behavior of the imino protons has been examined in greater detail by inversion–recovery methods and will be the subject of a separate paper.

Lastly, it is worth comparing these direct, more rigorous, assignments with earlier, less direct, methods. Previous methods for imino proton assignments have relied upon fragment studies, ring-current shift estimates, chemical modification, and paramagnetic ion binding, and we, and others, have used a combination of these methods in earlier attempts to assign a variety of tRNA species. In the case of *E. coli* $tRNA_1^{Val}$, we correctly deduced the assignments of the tertiary base pairs s^4U-8-A-14, G-19-C-56, m^7G-46-G-22, and G-15-C-48 (Reid et al., 1979; Hurd & Reid, 1979; Hurd et al., 1979). However, 10 of the 27 assignments made via these indirect methods are wrong in light of the present, more reliable assignments. As optimists, we prefer to consider it somewhat remarkable that 17 of the assignments were correct given the far less reliable techniques in those days. The major errors involving assignment discrepancies of over 0.5 ppm involve base pairs 6, 7, 11, and 13 and the tertiary base pair

T-54-A-58. The assignment of T-54 to peak F in $tRNA_1^{Val}$ is now unambiguous by three independent lines of evidence: (a) peak F, at 13.7 ppm in the presence of magnesium and 13.6 ppm at low magnesium, is a hydrogen-bonded N3-H from uridine or thymidine, and there is only one hydrogen-bonded N3-H in the entire T helix–loop region of $tRNA_1^{Val}$; (b) peak F is adjacent to the Ψ-55 peaks V and X (Figures 1, 2, and 6); (c) peak F is cross-saturated by a second-order steady-state NOE from the T-54 methyl resonance at 1 ppm (Figure 4). The 13.6–13.7 ppm assignment agrees with the assignment of T-54 in yeast $tRNA^{Phe}$ by Roy & Redfield, (1983) but differs markedly from the 12.46 ppm T-54 assignment of Hilbers et al. (1983) and Heerschap et al. (1983) in yeast $tRNA^{Phe}$. It is worth noting that Hilbers et al. relied upon a transient NOE from the thymine methyl to a multiple peak at 12.46 ppm to which GC-53 was already assigned. We routinely observe NOEs from the T-54 methyl resonance to GC-53, and it seems possible that they have misinterpreted the GC-53 NOE as T-54. Furthermore, the shorter steady-state saturation of the thymine methyl resonance in the presence of magnesium by Heerschap et al. revealed a discernible NOE to a peak at 13.7 ppm, which was ignored (Heerschap et al., 1983).

Given the fact that the previous indirect assignments for $tRNA_1^{Val}$, and undoubtedly other tRNAs, contain several errors, it is not surprising that attempts to monitor the thermal unfolding sequence and helix–coil dynamics in various portions of tRNA molecules have met with frustration and conflicting results.

References

Arter, D. B., & Schmidt, P. G. (1976) *Nucleic Acids Res. 3*, 1437.

Griffey, R. H., Poulter, C. D., Yamaizumi, Z., Nishimura, S., & Hurd, R. E. (1982) *J. Am. Chem. Soc. 104*, 5810.

Haasnoot, C. A. G., & Hilbers, C. W. (1983) *Biopolymers 22*, 1259.

Haasnoot, C. A. G., Heerschap, A., & Hilbers, C. W. (1983) *J. Am. Chem. Soc. 105*, 5483.

Hare, D. R. (1983) Ph.D. Thesis, University of California, Riverside, CA.

Hare, D. R., & Reid, B. R. (1982a) *Biochemistry 21*, 1835.

Hare, D. R., & Reid, B. R. (1982b) *Biochemistry 21*, 5129.

Hare, D. R., Wemmer, D. E., Chou, S. H., Drobny, G., & Reid, B. R. (1983) *J. Mol. Biol. 171*, 319.

Heerschap, A., Haasnoot, C. A. G., & Hilbers, C. W. (1982) *Nucleic Acids Res. 10*, 6981.

Heerschap, A., Haasnoot, C. A. G., & Hilbers, C. W. (1983a) *Nucleic Acids Res. 11*, 4483.

Heerschap, A., Haasnoot, C. A. G., & Hilbers, C. W. (1983b) *Nucleic Acids Res. 11*, 4501.

Hilbers, C. W., & Shulman, R. G. (1974) *Proc. Natl. Acad. Sci. U.S.A. 71*, 3239.

Hilbers, C. W., Heerschap, A., Haasnoot, C. A. G., & Walters, J. A. L. I. (1983) *J. Biomol. Struct. Dyn. 1*, 183.

Hurd, R. E., & Reid, B. R. (1979) *Biochemistry 18*, 4017.

Hurd, R. E., Azhderian, E., & Reid, B. R. (1979) *Biochemistry 18*, 4012.

Johnston, P. D., & Redfield, A. G. (1977) *Nucleic Acids Res. 4*, 3599.

Johnston, P. D., & Redfield, A. G. (1978) *Nucleic Acids Res. 5*, 3913.

Johnston, P. D., & Redfield, A. G. (1981) *Biochemistry 20*, 1147.

Kearns, D. R. (1976) *Prog. Nucleic Acid Res. Mol. Biol. 18*, 91.

Kim, S. H., Sussman, J. L., Suddath, F. L., Quigley, G. J., McPherson, A., Wang, A. H. J., Seeman, N. C., & Rich, A. (1974) *Proc. Natl. Acad. Sci. U.S.A. 71*, 4970.

Klug, A., Ladner, J., & Robertus, J. D. (1974) *J. Mol. Biol. 89*, 511.

Lightfoot, D. R., Wong, K. L., Kearns, D. R., Reid, B. R., & Shulman, R. G. (1973) *J. Mol. Biol. 78*, 71.

Macura, S., & Ernst, R. R. (1980) *Mol. Phys. 41*, 95.

Macura, S., Huang, Y., Suter, D., & Ernst, R. R. (1981) *J. Magn. Reson. 43*, 259.

Redfield, A. G. (1978) *Methods Enzymol. 49*, 253.

Reid, B. R., Ribeiro, N. S., McCollum, L., Abbate, J., & Hurd, R. E. (1977) *Biochemistry 16*, 2086.

Reid, B. R., McCollum, L., Ribeiro, N. S., Abbate, J., & Hurd, R. E. (1979) *Biochemistry 18*, 3996.

Robillard, G. T., Tarr, C. E., Vosman, F., & Berendsen, H. J. C. (1976) *Nature (London) 262*, 363.

Romer, R., & Varadi, V. (1977) *Proc. Natl. Acad. Sci. U.S.A. 74*, 1561.

Roy, S., & Redfield, A. G. (1981) *Nucleic Acids Res. 9*, 7073.

Roy, S., Papastavros, M. Z., & Redfield, A. G. (1982) *Biochemistry 21*, 6081.

Salemink, P. J. M., Yamane, T., & Hilbers, C. W. (1977) *Nucleic Acids Res. 4*, 3737.

Scheek, R. M., Russo, N., Boelens, R., Kaptein, R., & van Boom, J. H. (1983) *J. Am. Chem. Soc. 105*, 2914.

Shulman, R. G., Hilbers, C. W., Kearns, D. R., Reid, B. R., & Wong, Y. P. (1973) *J. Mol. Biol. 78*, 57.

Teitelbaum, H., & Englander, S. W. (1975) *J. Mol. Biol. 92*, 79.

Tropp, J., & Redfield, A. G. (1981) *Biochemistry 20*, 2133.

Wagner, G., & Wuthrich, K. (1982) *J. Mol. Biol. 155*, 347.

Wemmer, D. E., Chou, S.-H., Hare, D. R., & Reid, B. R. (1984) *Biochemistry 23*, 2262.

Wuthrich, K., Wider, G., Wagner, G., & Braun, W. (1982) *J. Mol. Biol. 155*, 311.